Phytochemistry 69 (2008) 2426–2438

Contents lists available at ScienceDirect

Phytochemistry

journal homepage: www.elsevier.com/locate/phytochem

# Proteomic analysis of soybean nodule cytosol

Nathan W. Oehrle [a], Annamraju D. Sarma [b], James K. Waters [c], David W. Emerich [b,*]

[a] United States Department of Agriculture, Curtis Hall, University of Missouri, Columbia, MO 65211, United States
[b] Department of Biochemistry, 117 Schweitzer Hall, University of Missouri, Columbia, MO 65211, United States
[c] Agricultural Experiment Station Chemical Laboratories, 4 Agriculture Building, University of Missouri, Columbia, MO 65211, United States

ARTICLE INFO

*Article history:*
Received 10 April 2008
Received in revised form 24 June 2008
Available online 29 August 2008

*Keywords:*
*Glycine max*
Leguminosae
Proteomics
Soybean
Nodules
*Bradyrhizobium japonicum*
Glycolysis
2D Electrophoresis
Mass spectrometry

ABSTRACT

An isolation procedure for soybean (*Glycine max* L. cv Williams 82) nodule cytosol proteins was developed which greatly improved protein resolution by two-dimensional polyacrylamide gel electrophoresis. The most abundant proteins were selected and analyzed by mass spectrometry. The identified proteins were categorized by function (% of total proteins analyzed): carbon metabolism (28%), nitrogen metabolism (12%), reactive oxygen metabolism (12%) and vesicular trafficking (11%). The first three categories were expected based on the known physiological functions of the symbiotic nitrogen fixation process. The number of proteins involved in vesicular trafficking suggests a very active exchange of macromolecules and membrane components. Among the 69 identified proteins were the enzymes of the three carbon portion of glycolysis, which were further characterized to support their roles in the sucrose synthase pathway to provide malate for the bacteroids. Proteomic analysis provides a functional tool by which to understand and further investigate nodule function.



## 1. Introduction

Soybean has the ability to undergo a symbiotic interaction with the soil microorganism, *Bradyrhizobium japonicum*, to form a nitrogen-fixing symbiosis. The symbiosis takes the form of tumor-like growths, referred to as nodules, on the roots of the plant. The structural organization of legume nodules is quite complex, composed of different zones and various cell types each with different functional attributes (Brown and Walsh, 1994). Determinant, or spherical nodules, such as those found on soybean do not have persistent meristems. The vascular system becomes closed conferring a continuous system of vascular branches, and there is little or no involvement of infection threads in the distribution of bacteria into nodule cells. Determinate nodules are developmentally synchronized; that is, they contain only one specific developmental form dictated by the age of the nodule. The central portion of a determinant nodule is interspersed with smaller infected and larger uninfected cells resulting in approximately 1.6 uninfected cells for each infected cell (Newcomb and Tandon, 1981). Within each infected cell of determinate-type soybean nodules, the *B. japonicum* bacteroids are distributed within membrane envelopes called symbiosomes (Roth et al., 1988). The bacteroids never come into direct contact with the host cell cytoplasm as the symbiosome membrane acts as a selective permeability barrier for the transport of plant metabolites to the bacteroids and fixed nitrogen to the plant (Udvardi and Day, 1997).

A number of specific plant proteins, referred to as nodulins, are expressed during infection, nodule maturation and maintenance to support the nitrogen fixation process (Sánchez et al., 1991). Enzymatic analyses have identified additional plant proteins that participate in the process. The complexity of the process suggests that a multitude of proteins have yet to be identified and characterized. Global analytical procedures have been applied to nodules of leguminous plants. For example, in *Medicago truncatula* nodules, of the 765 identified genes that were differentially expressed during the nodulation process, 41 were previously known nodulation genes, indicating that global analysis had revealed hundreds of additional genes (El Yahyaoui et al., 2004). In agreement with biochemical reports, genes for sucrose synthase, β-amylase, a hexose transporter, glycolytic enzymes, malate dehydrogenase and PEPC are up-regulated in nodules (Colebatch et al., 2004; El Yahyaoui et al., 2004; Kouchi et al., 2004; Tesfaye et al., 2006).

Lee et al. (2004) constructed a cDNA microarray of 382 selected clones of genes selected as up-regulated in soybean root nodules. Among the 81 genes found to be differentially expressed during nodule development were 18 previously known nodulins. The nodulins constituted the largest group of functionally categorized proteins. Other differentially expressed genes included those in amino acid metabolism (cysteine synthase, tyrosine aminotransferase),

* Corresponding author. Tel.: +1 573 882 4252; fax: +1 573 882 5635.
*E-mail address:* EmerichD@Missouri.edu (D.W. Emerich).

0031-9422/$ - see front matter © 2008 Elsevier Ltd. All rights reserved.
doi:10.1016/j.phytochem.2008.07.004

vitamin metabolism (thiamin biosynthetic enzyme, coproporphyrinogen oxidase, nicotinamide aminotransferase B) and signal transduction (remorin 1, 14-3-3-like protein, inositol 1,3,4-trisphosphate 5/6-kinase protein).

Bestel-Corre et al. (2002) reported proteomic analysis of *M. truncatula* inoculated with either the nitrogen-fixing *Sinorhizobium meliloti* or the mycorrhizal fungus *Glomus mosseae*. Among the symbiosis-related proteins were elongation factor Tu, enolase, and leghemoglobin. In addition, proteins from *S. meliloti* were identified: malate dehydrogenase and superoxide dismutase. Wan et al. (2005) have used proteomics to identify proteins in the root hairs after infection by *B. japonicum*. Root hair protein preparations were obtained after 0, 3, 6, and 12 h exposure to *B. japonicum*. They found proteins previously identified as known to respond to rhizobial inoculation such as lipoxygenases, agglutinin, actin, peroxidase and phenylalanine ammonia lyase, but also identified novel proteins such as phospholipase D and phosphoglucomutase. A small protein proteome of *M. truncatula* nodules establishes the presence of ribosomal proteins S6 and L24, a histone-like protein and a peroxidase precursor (Zhang et al., 2006). Larrainzar et al. (2007) identified 377 *M. truncatula* plant nodule proteins. The largest number of proteins identified were functionally grouped as in amino acid metabolism (12%), redox and stress (12%) and glycolysis (12%).Here we report a proteomic analysis of the cytosol from mature soybean nodules and found that the majority of the 69 identified proteins were enzymes of carbon, nitrogen and oxygen metabolism and proteins involved in protein trafficking.

## 2. Results and discussion

### 2.1. Protein categories and locations

A whole proteome analysis of soybean nodule cytosol was undertaken using two-dimensional protein separation followed by peptide mass fingerprinting. Current protein isolation techniques for plant tissue samples did not provide adequate separation (Kersten et al., 2002), so a protocol specific for soybean nodule cytosol was designed based on those techniques (Section 4). The modification of the protein isolation procedure greatly improved the resolution of proteins during separation (Fig. 1). Selection of proteins for analysis was random but biased toward the most highly abundant proteins of the soybean nodule cytosol proteome. Of the several hundred spots extracted from the gel, only 69 (Fig. 1) gave confident identities in the soybean UniGene database (Mooney and Thelen, 2004). Many spectra matched only clones with no ascribed function (data not shown).

The largest categories of proteins was that defined as those involved in carbon metabolism (~28%) followed by nitrogen metabolism (~12%), oxygen protection (~12%), and protein trafficking (11%). The first three categories define the primary metabolic activities of the nodule and as such together constitute more than half of all the proteins identified. Although classified somewhat differently, these three largest categories were similar to those reported by Larrainzar et al. (2007) in *M. truncatula* nodules. The number of proteins involved in vesicular trafficking suggests a very active exchange of macromolecules larger than the carbon and nitrogen metabolites known to be exchanged that form the basis of the symbiosis. Proteins known to be in either infected cells or uninfected cells were found. For example, sucrose synthase (spot 22) has been reported to be present in greater abundance in the infected cells whereas glutamine synthetase (spots 3 and 4) and aspartate aminotransferase (spot 10) were more abundant in uninfected cells (Kouchi et al., 1988; Zammit and Copeland, 1993). Urate oxidase (spot 8) has been localized to the peroxisomes of infected cells (Nguyen et al., 1985). Ascorbate peroxidase (spots 5 and 6) (Dalton et al., 1993) was found in the cytoplasm of both infected and uninfected nodule cells.

### 2.2. Proteomic and transcriptomic similarities

A number of proteins were found both in the soybean proteome (Fig. 1) as reported here and as mRNAs in the soybean transcriptome as reported by Lee et al. (2004) including sucrose synthase

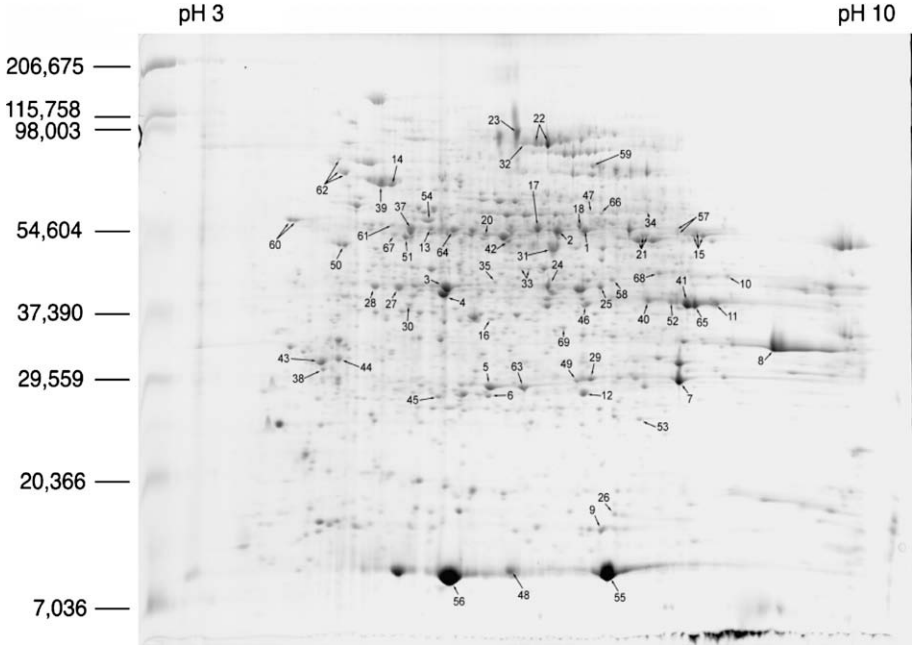


**Fig. 1.** Image of two-dimensional SDS–PAGE of the plant cytosolic fraction of soybean nodules. Those proteins considered most abundant were chosen for mass spectral analysis. The proteins catalogued on this image are described in Table 1. IEF was performed using a 24 cm, 3–10 linear IPG strip. The second dimension separation utilized a 10–18% gradient of acrylamide. Gel was run, proteins isolated and analyzed as described in detail in Section 4.

**Table 1**
PMF matching of soybean nodule cytosol proteins

| Spot # Protein Name/EC # Accession # | MOWSE or Mascot score | # Hit/# submitted | % Coverage | p*I* theoretical | p*I* experimental | MW (kDa) Theoretical | MW (kDa) Experimental |
|---|---|---|---|---|---|---|---|
| Spot # 1 Enolase 4.2.1.11 (putative) Soybean UniGene Gma# S4964672 | 5.00E+5 | 7/42 | 58 | 5.42 (*Oryza sativa*) | 6.80 | 48 (*O. sativa*) | 60 |
| Spot # 2 Enolase 4.2.1.11 (putative) Soybean UniGene Gma# 4964672 | 5.00E+5 | 7/28 | 58 | 5.54 (*Arabidopsis thaliana*) | 7.10 | 48 (*A. thaliana*) | 60 |
| Spot # 3 Glutamine synthetase 6.3.1.2 Soybean UniGene Gma# S5146672 | 2.05E+5 | 7/18 | 15 | 5.68 | 5.65 | 39 | 42 |
| Spot # 4 Glutamine synthetase 6.3.1.2 Soybean UniGene Gma# S5146672 | 1.55E+8 | 10/17 | 32 | 5.5 | 5.6 | 39 | 40 |
| Spot # 5 Ascorbate peroxidase 1.11.1.11[a] Soybean UniGene Gma# S5146810 | 4.11E+6 | 9/15 | 48 | 5.51 | 6.0 | 27–30 | 28.5 |
| Spot # 6 Ascorbate peroxidase 2 Soybean UniGene Gma# S5146757 | 6.23E+8 | 11/18 | 57 | 5.65 | 6.4 | 27.1 | 28.6 |
| Spot # 7 Acid phosphatase 3.1.3.2 Soybean UniGene Gma# S5146353 | 588,000 | 9/29 | 42 | 6.86 | 8.0 | 30.1 | 31 |
| Spot # 8 Nodulin 35[b] Soybean UniGene Gma# S5146658 | 2.42E+10 | 14/20 | 61 | 8.31 | 8.9 | 35 | 33 |
| Spot # 9 Nucleoside diphosphate kinase 2.7.4.6 Gma# S5146781 | 3.39E+4 | 4/11 | 23 | 5.93 | 7.2 | 16.3 | 15 |
| Spot # 10 Aspartate aminotransferase 2.6.1.1 Soybean UniGene Gma# S5146543 | 2.99E+4 | 7/78 | 58 | 8.67 | 7.1/8.3 | 49.7 | 44.3/44.8 |
| Spot # 11 NADP-Isocitrate dehydrogenase 1.1.1.42 Soybean UniGene Gma# S5146471 | 2.45E+3 | 6/55 | 15 | 5.87 | 8.4 | 46 | 40 |
| Spot # 12 31 kDa protein Soybean UniGene Gma# S5146880 | 7.15E+3 | 7/44 | 26 | 8.64 | 7.0 | 28.8 | 31 |
| Spot # 13 Unknown protein Soybean UniGene Gma# S5146701 | 4.71E+9 | 17/91 | 28 | – | 4.9 | – | 55 |
| Spot # 14 Maturation peptide Soybean UniGene Gma# S5146850 | 7.97E+5 | 14/87 | 25 | – | 4.9 | – | 74.2 |
| Spot # 15 Catalase 1.11.1.6 Soybean UniGene Gma# 5146605 | 1.11E+13 | 17/53 | 32 | 6.77 | 8.0 | 57 | 53 |
| Spot # 16 Unknown protein Soybean UniGene Gma# S4933200 | 5.45E+3 | 4/28 | 51 | – | 6.1 | – | 37 |
| Spot # 17 Inosine monophosphate dehydrogenase 1.1.1.205 Soybean UniGene Gma# S5146502 | 4.02E+13 | 22/75 | 50 | 5.6 | 6.5 | 53.4 | 54.3 |
| Spot # 18 Inosine monophosphate dehydrogenase (Mascot) NCBI GenBank CAB38030 | 86/75 | 15/75 | 47 | 5.54 | 6.9 | 53.4 | 56.5 |
| Spot # 19 Resistance protein KR1 Soybean UniGene Gma# S5146195 | 3.78E+5 | 12/75 | 15 | – | 7.6 | – | 79.2 |
| Spot # 20 Selenium binding protein Soybean UniGene Gma# S5146283 | 1.18E+16 | 25/75 | 53 | 5.62 | 6.0 | 53.4 | 52.3 |

**Table 1** (*continued*)

| Spot # Protein Name/EC # Accession # | MOWSE or Mascot score | # Hit/# submitted | % Coverage | p*I* theoretical | p*I* experimental | MW (kDa) Theoretical | MW (kDa) Experimental |
|---|---|---|---|---|---|---|---|
| Spot # 21 Serine hydroxymethyl transferase 2.1.2.1 Soybean UniGene Gma# S4891713 | 2.12E+6 | 9/75 | 23 | 7.2 | 7.58 | 55 (*A. thaliana*) | 51.2 |
| Spot # 22 Sucrose synthase 2.4.1.13[c] Soybean UniGene Gma# S5146556 | 2.65E+25 | 40/75 | 49 | 6.04 | 6.6 | 92 | 91.7 |
| Spot # 23 Lipoxygenase 1.13.11.12 Soybean UniGene Gma# S5146889 | 1.22E+25 | 38/75 | 48 | 5.78 | 6.34 | 96 | 96.3 |
| Spot # 24 3-Phosphoglycerate kinase 2.7.2.3 Soybean UniGene Gma# S4878044 | 2.74E+4 | 6/31 | 34 | 5.73 (*Pisum sativum*) | 6.6 | 43 (*P. sativum*) | 42.3 |
| Spot # 25 3-Phosphoglycerate kinase 2.7.2.3 Soybean UniGene Gma# S4878044 | 1.53E+6 | 8/36 | 43 | 5.73 (*P. sativum*) | 7.1 | 43 (*P. sativum*) | 42.5 |
| Spot # 26 ADP-ribosylation factor Soybean UniGene# S5146515 | 8.44E+5 | 10/46 | 58 | 6.42 | 7.3 | 20.4 | 16.4 |
| Spot # 27 Clathrin (heavy chain) Soybean UniGene Gma# S5146549 | 4.70E+8 | 14/75 | 12 | 5.37 | 5.1 | 193 | 42.9 |
| Spot # 28 Alternative oxidase Soybean UniGene Gma# S5146594 | 192/75 | 4/28 | 23 | – | 4.8 | – | 43 |
| Spot # 29 31 kDa protein Soybean UniGene Gma# S5146880 | 3.71E+8 | 12/54 | 44 | 8.64 | 7.1 | 28.8 | 29.1 |
| Spot # 30 Fatty acid epoxide hydrolase Soybean UniGene Gma# S6672296 | 8.60E+10 | 16/65 | 65 | 5.43 | 5.2 | 39 | 39.2 |
| Spot # 31 NAD(P)H-Isocitrate dehydrogenase Soybean UniGene Gma# S5146549 | 1.2E+11 | 17/51 | 31 | 5.87 | 6.0 | 46 | 48 |
| Spot # 32 Lipoxygenase Soybean UniGene Gma# S5146889 | 1.32E+22 | 33/75 | 49 | 5.78 | 6.4 | 96 | 93.3 |
| Spot # 33 Glutamate 1-semialdehyde aminotransferase 5.4.3.8 Soybean UniGene Gma# S5146856 | 2.29E+5 | 10/22 | 44 | 5.7 | 6.3 | 46 | 44.4 |
| Spot # 34 Ferric leghemoglobin reductase-2 precursor[d] Soybean UniGene Gma# S5146201 | 6.10E+3 | 7/42 | 17 | 6.91 | 7.66 | 53 | 61.3 |
| Spot # 35 440 Gmax SC Soybean UniGene Gma# S4997797 | 1.60E+3 | 5/23 | 34 | – | 6.1 | – | 43.6 |
| Spot # 36 Isoflavone reductase (homolog 2) Soybean UniGene Gma# S5146432 | 1.94E+13 | 17/51 | 58 | 5.6 | 6.0 | 35 | 36.7 |
| Spot # 37 4-Coumarate-CoA ligase 6.2.1.12 (pathogen resistance) Soybean UniGene Gma# S5146211 | 1.42E+4 | 11/75 | 12 | 6.2 | 5.2 | 60 | 54 |
| Spot # 38 14-3-3 protein Soybean UniGene Gma# 5146682 | 9.26E+2 | 6/33 | 41 | 4.71 | 4.41 | 29 | 30.3 |
| Spot # 39 Heat shock protein (Mascot) NCBI GenBank AAV98051 | 90/75 | 15/59 | 34 | 5.08 (*Medicago sativa*) | 4.91 | 71.4 (*M. sativa*) | 74.3 |
| Spot # 40 NAD-Glyceraldehyde-3-$PO_4$ dehydrogenase (Mascot) NCBI GenBank ABC75834 | 76/75 | 11/46 | 38 | 6.72 | 7.6 | 37 | 40.5 |

(*continued on next page*)

**Table 1** (*continued*)

| Spot # Protein Name/EC # Accession # | MOWSE or Mascot score | # Hit/# submitted | % Coverage | p*I* theoretical | p*I* experimental | MW (kDa) Theoretical | MW (kDa) Experimental |
|---|---|---|---|---|---|---|---|
| Spot # 41<br>NAD-Glyceraldehde-3-$PO_4$ dehydrogenase (Mascot)<br>NCBI GenBank ABC75834 | 78/75 | 12/54 | 37 | 6.72 | 8.1 | 37 | 39.6 |
| Spot # 42<br>53 kDa Nodulin (Mascot)<br>NCBI GenBank AAC72337 | 75/75 | 15/60 | 40 | 5.74 | 6.2 | 52 | 51.6 |
| Spot # 43<br>14-3-3 like protein (Mascot)<br>NCBI GenBank CAA88415 | 102/75 | 14/54 | 55 | 4.71 (*Vicia faba*) | 4.3 | 30 (*V. faba*) | 31.8 |
| Spot # 44<br>14-3-3 like protein<br>Soybean UniGene Gma# S5146682 | 5.44E+7 | 11/43 | 23 | 4.71 | 4.5 | 30 | 31.6 |
| Spot # 45<br>Fe-superoxide dismutase (Mascot)<br>NCBI GenBank AAQ13492 | 62/67 | 12/75 | 47 | 5.45 | 5.5 | 28 | 27.8 |
| Spot # 46<br>Malate dehydrogenase (Mascot)<br>Soybean UniProtKB Q9SPB8 | 4.62E+5 | 16/194 | 44 | 8.2 | 7 | 36.2 | 39.3 |
| Spot # 47<br>Nitrogenase β-chain from *B. japonicum* 110 (Mascot)<br>NCBI GenBank AAA26326 | 91/74 | 16/73 | 64 | 6.1 | 7.1 | 57.8 | 61 |
| Spot # 48<br>Leghemoglobin A, Nodulin 2 (Mascot)<br>NCBI GenBank CAA23731 | 100/75 | 9/33 | 75 | 6.1 | 6.25 | 15.3 | 10.2 |
| Spot # 49<br>Vegetative storage protein b (Mascot)<br>Soybean UniGene Gma# S5146880 | 3.70E+8 | 12/54 | 44 | 6.72 | 7.0 | 29 | 29.4 |
| Spot # 50<br>Apyrase 3.6.1.5 [early nodulin] (Mascot)<br>NCBI GenBank AAG32959 | 88/75 | 13/44 | 26 | 5 | 4.5 | 52 | 51 |
| Spot # 51<br>Gro EL3 chaperonin from *B. japonicum* 110 (Mascot)<br>NCBI GenBank P35862 | 64/75 | 16/75 | 36 | 5.2 | 5.2 | 57 | 52.2 |
| Spot # 52<br>Glyceraldehyde-3-$PO_4$-dehydrogenase (Mascot)<br>NCBI GenBank ABC75834 | 120/66 | 19/172 | 58 | 6.8 | 8.0 | 36.9 | 42 |
| Spot # 53<br>Mn-superoxide dismutase (Mascot)<br>NCBI GenBank CAD29434 | 70/66 | 11/264 | 75 | 6.1 | 7.6 | 16 | 24 |
| Spot # 54<br>Gro EL3 chaperonin from *B. japonicum* (Mascot)<br>NCBI GenBank CH603_BRAJA | 181/75 | 28/75 | 54 | 5.2 | 5.4 | 57.6 | 54.3 |
| Spot # 55<br>Leghemoglobin A (Mascot)<br>NCBI GenBank CAA23731 | 121/66 | 10/56 | 78 | 6.1 | 7.2 | 15.3 | 10.1 |
| Spot # 56 | | | | | | | |
| Leghemoglobin C1 [Nodulin 50] (Mascot)[e] | 82/66 | 7/53 | 75 | 5.37 | 5.6 | 15.3 | 10.1 |
| Leghemoglobin C2 [Nodulin 50] (Mascot) | 83/66 | 7/53 | 62 | 5.38 | 5.6 | 15.5 | 10.1 |
| Leghemoglobin C3 [Nodulin 50] (Mascot)<br>NCBI GenBank CAA23730, AAA33980, CAA23732 | 116/66 | 9/53 | 78 | 5.36 | 5.6 | 15.5 | 10.1 |
| Spot # 57<br>ATP synthase, α-chain (Mascot)<br>NCBI GenBank CAA78407 | 152/75 | 23/70 | 53 | 6.3 | 7.9 | 55 | 54 |
| Spot # 58<br>Coproporphyrinogenase (Mascot)<br>NCBI GenBank CAA50401 | 182/75 | 18/34 | 59 | 6.7 | 7.3 | 43 | 44.2 |
| Spot # 59<br>Methionine synthase (Mascot)<br>NCBI GenBank AAQ08403 | 159/66 | 29/166 | 39 | 5.93 | 7.1 | 84.4 | 82.8 |

**Table 1** (*continued*)

| Spot # Protein Name/EC # Accession # | MOWSE or Mascot score | # Hit/# submitted | % Coverage | p*I* theoretical | p*I* experimental | MW (kDa) Theoretical | MW (kDa) Experimental |
|---|---|---|---|---|---|---|---|
| Spot # 60 α-carboxyltransferase Soybean UniGene Gma# S5146688 | 3770 | 7/24 | 15 | 7.64 | 4.0 | 78 | 58 |
| Spot # 61 ATP-ase β-chain (Mascot) NCBI GenBank AAA70268 | 70/66 | 11/71 | 28 | 6 (*Zea mays*) | 5.1 | 59 (*Z. mays*) | 55 |
| Spot # 62 Heat shock protein (Mascot) NCBI GenBank CAA52149 | 84/75 | 13/61 | 20 | 5.1 (*Cucumis sativus*) | 4.6 | 75.5 (*Cu. sativus*) | 79 |
| Spot # 63 Carbonic anhydrase 4.2.1.1 Soybean UniGene Gma# S5146415 | 3270 | 7/44 | 37 | 6.25 | 6.4 | 29.7 | 28.6 |
| Spot # 64 β-amylase (Mascot) NCBI GenBank AAA33941 | 62/75 | 16/91 | 30 | 5.3 | 5.6 | 55 | 54 |
| Spot # 65 Glyceraldehye-3-$PO_4$-dehydrogenase (Mascot) NCBI GenBank ABC75834 | 131/66 | 22/209 | 56 | 6.72 | 8.0 | 36.9 | 39 |
| Spot # 66 Nitrogenase β-chain from *B. japonicum* 110 (Mascot) NCBI GenBank NP_768384 | 126/78 | 24/156 | 62 | 6.1 | 7.3 | 57.8 | 61 |
| Spot # 67 ATP synthase β-chain from *B. japonicum* 110 (Mascot) NCBI GenBank NP_767080 | 140/67 | 30/244 | 77 | 5.13 | 5.2 | 51 | 52.5 |
| Spot # 68 1-aminocyclopropane-1-carboxylate deaminase from *B. japonicum* 110 (Mascot) NCBI GenBank NP_766881 | 124/52 | 23/220 | 81 | 6.34 | 7.55 | 36.5 | 39 |
| Spot # 69 Nod factor transporter from *B. japonicum* 110 (Mascot) NCBI GenBank NP_768670 | 50/55 | 9/82 | 36 | 7.05 | 7.15 | 34.6 | 35 |

[a] Immunolocalized to cytoplasm of infected and uninfected cells (Dalton et al., 1993).
[b] Immunolocalized to the peroxisome of uninfected cells (Van den Bosch and Newcomb, 1985; Dalton et al., 1993).
[c] Immunolocalized to cytoplasm, predominately uninfected cells (Gordon et al., 1992).
[d] Immunolocalized to mitochondria, cytosol and bacteroids (Moran et al., 2002).
[e] Immunolocalized to cytoplasm and nucleus of infected and uninfected cells (Vandenbosch and Newcomb, 1988).

(spot 22), nodulin 35 (spot 8), coproporphyrinogenase (spot 58), ferric leghemoglobin reductase-2 (spot 34) and leghemoglobins A (spot 55) and C (spot 56). In addition, homologues of 14-3-3 proteins (spots 38, 43, and 44) and resistance proteins (spot 19) were identified both as proteins as reported here and as transcripts as reported by Lee et al. (2004). The fact that these were identified both in the proteome (Fig. 1) and in the transcriptome (Lee et al., 2004) suggest these proteins perform a critical role in nodule functioning.

### 2.3. Oxygen metabolism

Leghemoglobins A (spot 55) and C (spot 56) were among the most prominent proteins observed. Ferric leghemoglobin reductase-2 (spot 34) which maintains the iron of leghemoglobin in its active ferrous state (Lin et al., 1991) was also identified. Ascorbate peroxidase (spots 5 and 6), catalase (spot 15), Fe-superoxide dismutase (spot 45) and Mn-superoxide dismutase (spot 53) perform roles in scavenging active oxygen species. In contrast, a single Fe-superoxide dismutase was identified in the *B. japonicum* bacteroid proteome (Sarma and Emerich, 2005). Consistent with the need for oxygen protection and supply, coproporphyrinogenase (spot 58) was found in both the proteome and the transcriptome (Lee et al., 2004). Coproporphyrinogenase catalyzes the conversion of coproporphyrinogen III to protoporphyrinogen IX in the heme biosynthesis pathway. The resulting heme provides components for leghemoglobin, catalase and ascorbate peroxidase which were also identified as prominent proteins as well as for cytochromes for electron transport and energy formation. Hoa et al. (2004) found coproporphyrinogenase localized only in mitochondria within nodules of soybean indicating the soybean nodule cytosol contained detectable levels of mitochondrial proteins. Further testament to the importance of heme metabolism and maintenance was glutamate-semialdehyde aminotransferase (spot 33) which catalyzes the conversion of [*S*]-4-amino-5-oxopentanoate to 5-aminolevulinate an early step in heme biosynthesis.

### 2.4. Nitrogen metabolism

Glutamine synthetase (spots 3 and 4), aspartate aminotransferase (spot 10), and inosine monophosphate dehydrogenase (spots 17 and 18) are enzymes involved in ureide biosynthesis. Ureides are the major nitrogen assimilation product of soybean nodules transported to the shoot. Curiously, only one of the enzymes of ureide biosynthesis, succinoaminoimidazolecarboximide ribonucleotide synthetase, was found in the transcriptome (Lee et al., 2004). Several additional enzymes of amino acid metabolism were identified in the proteome, serine hydroxymethyltransferase (spot 21) and methionine synthase (spot 59), and the transcriptome, cysteine synthase and tyrosine aminotransferase (Lee et al., 2004). Soybean nodule bacteroids were shown to have the ability to synthesize a number of amino acids (Sarma and Emerich, 2005). The ability of both symbionts to metabolize amino acids provides support for nutrient exchange cycles (Lodwig et al., 2003).

### 2.5. Fatty acid signaling

Lipoxygenase (spots 23 and 32) and fatty acid epoxide hydroxylase (spot 30) were both highly expressed proteins. Lipoxygenase activity has been documented in soybean root nodules previously (Junghans et al., 2004; Mohammadi and Karr, 2003) but not the presence of fatty acid epoxide hydroxylase. The expression of lipoxygenase and fatty acid epoxide hydrolase would provide an alternative metabolic route for hydroperoxides formed by lipoxygenase instead of pathways for the biosynthesis of traumatic acid or jasmonic acid. Traumatic acid is a member of a large class of alkenals which are toxic natural products of fatty acid oxidation (Farmer, 1994) Jasmonic acid is a key regulator in the development, physiology, and defense of plants and is involved in carbon partitioning and mechanotransduction (Wasternack and Hause, 2002). Fatty acid epoxide hydrolase may perform a role in the developmental synchrony and/or senescence of soybean nodules. Fatty acid epoxide hydrolase occurs after the branchpoint by which 13-hydroperoxylinolenic acid is either cleaved by hydroperoxide lyase to *cis*-3-hexenal and 12-oxo-*cis*-9-dodecenoic acid, the later of which is isomerized to traumatic acid (12-oxo-*trans*-10-dodecenoic acid) or converted by allene oxide synthase to 12,13-epoxylinolenic acid. This later compound can be metabolized through a series of rearrangement, cyclization, reduction and β-oxidation steps to form jasmonic acid.

### 2.6. Nodulins

Nodulins are plant-genome-encoded proteins exclusively or highly up-regulated in nodules upon infection with rhizobia. A number of known nodulins were identified; sucrose synthase (spot 22), urate oxidase (spot 8), ferric leghemoglobin reductase (spot 34), apyrase (spot 50), leghemoglobin A (spots 48 and 55) and leghemoglobin C (spot 56). Panter et al. (2000) noted that Nodulin 53 was identified as a 31 kDa protein presumably via proteolysis and speculated that it was processed to serve a discrete function. The 31 kDa protein identified here (spots 12 and 20) was similar to Nodulin 53 confirming the observations of Panter et al. (2000). Nodulin 53 is a symbiosome membrane associated protein which shows that these compartmentalized proteins are represented in the cytosolic proteome. Panter et al. (2000) identified Nodulin 53 as one of 17 proteins associated with the symbiosome membrane of soybean root nodules. Nodulin 53 was not predicted to have a transmembrane domain, but it may be anchored to the symbiosome membrane via myristoylation (Winzer et al., 1999).

### 2.7. Nucleoside/nucleotide-requiring proteins

A number of proteins that required nucleosides and nucleotides were found: nucleoside diphosphate kinase (spot 9), ATP synthase (spot 57), ATPase β-chain (spot 61) and apyrase (spot 50). The nucleoside diphosphate kinase was identical to that first reported by Krishnan et al. (1999) in the exudate from imbibing seed and matches the NDPK type I clones in the soybean databases (e.g. AW100564). The energy demands of nitrogen fixation require a capacity to maintain ATP concentrations via ATP synthase and nucleoside diphosphate kinase. The presence of NDPK type I in both germinating seeds and nodules substantiates the extensive roles this enzyme performs in energy metabolism.

### 2.8. Vegetative storage proteins

The vegetative storage proteins (spot 49) normally found in protein bodies are lysine-rich glycoproteins first identified in the leaves of soybean (Wittenbach, 1982) and have subsequently been found in other plant organs and ascribed potential metabolic roles (Meuriot et al., 2004; Penheiter et al., 1997; Tranbarger et al., 1991) as well as nitrogen storage. In soybean, the lower molecular weight vegetative storage proteins have homology to acid phosphatases (Staswick, 1989; Penheiter et al., 1997) and the high MW vegetative storage proteins have similarity to lipoxygenase (Tranbarger et al., 1991). The low molecular weight vegetative storage protein (VSP) differs most strikingly from the acid phosphatases (spot 7) in the substitution of a serine in place of the conserved nucleophilic aspartate residue in the N terminus, which renders it function as a phosphatase. Leelapon et al. (2004) reported that a single amino acid substitution in soybean vegetative storage protein α increased its acid phosphatase activity about 20-fold. Bonefide acid phosphatases that are closely related to VSPs are also found in soybean nodules (Penheiter et al., 1997). In *Medicago sativa* taproots, methyl jasmonate alters expression of the low molecular weight vegetative storage proteins (Meuriot et al., 2004). As mentioned above, fatty acid epoxide hydrolase may partition 13-hydroperoxylinolenic acid to form jasmonic acid and thus regulate vegetative storage proteins in soybean.

### 2.9. B. japonicum proteins

Several proteins from *B. japonicum* were identified among the selected nodule cytosol proteins; the β-chain of nitrogenase MoFe–protein (spots 47 and 66), the ATPase β-chain (spot 67), 1-aminocylcopropane-1-carboxylate deaminase (spot 68), the Nod factor transporter (spot 69), and the chaperonin GroEL3 (spots 51 and 54), which are abundant proteins within the microsymbiont. Catalano et al. (2004) found 23 bacterial proteins among the symbiosome membrane proteins of *M. truncatula* root nodules. Wienkoop and Saalbach (2003) analyzed the proteome of symbiosome membranes from *Lotus japonicus* root nodules and found the Fe protein of nitrogenase and 13 other bacteroid proteins. Panter et al. (2000) found a number of unknown proteins associated with the symbiosome membrane of soybean root nodules. Their work was published prior to the sequencing of the *B. japonicum* genome. Analysis of their seven proteins with no homology to known proteins indicated that protein 17 was homologous to *B. japonicum* gene blr1311, an outer membrane protein and that protein 56/57 was homologous to *B. japonicum* genes bll4354, blr4699, blr4700, blr 4701, blr4867, blr4994, blr5174 and blr 7695, which were identified as outer membrane or hypothetical proteins. These results emphasize the technical difficulties in separating the symbionts and their component macromolecules for analysis.

### 2.10. Vesicular proteins

A number of vesicular proteins were identified which may be involved in symbiosome membrane generation. In soybean root nodules, almost 30 times more membrane is generated in the form of symbiosome membrane than plasma membrane (Winzer et al., 1999). The symbiosome membrane is derived from the host plasma membrane that surrounds the infection thread at the time of release of bacteria into the host cell. Following endocytosis, this membrane undergoes significant changes in composition (Verma and Hong, 1996). Proteins to the symbiosome membrane and symbiosome space are delivered via vesicles from the Golgi (Cheon et al., 1993; Kinnback et al., 1987).

Clathrin (spots 27 and 28) and ADP-ribosylation factor (spot 26) were identified which supports active exchange of macromolecules and membrane components between the infected and non-infected nodule cells and perhaps between the two symbionts. Clathrin is the major protein of the polyhedral layer of coated pits and vesicles formed during endocytosis of materials at the surface of cells (Brodsky et al., 2001; Jürgens, 2004). Two different adaptor protein complexes link the clathrin lattice either to the plasma

membrane or to the trans-Golgi network. ADP-ribosylation factors are 20 kDa GTP-binding proteins involved in protein trafficking which are members of the Ras superfamily of regulatory GTP-binding proteins (Memon, 2004) and regulate metabolism via 14-3-3 (spots 38, 43, and 44) gene activation (Zuk et al., 2003). In addition, enolase (spots 1 and 2), a cytosolic enzyme of glycolysis, has been found bound to the vacuoles and has been reported to activate homotypic vacuole fusion and protein transport to the vacuole in yeast (Decker and Wickner, 2006). A number of glycolytic enzymes have cellular functions in addition to their roles in glycolysis (Kim and Dang, 2005). Selenium-binding protein (spot 20) is one of the cytosolic proteins which is believed to bind to selenium without containing selenocysteine. Although its physiological role remains to be identified, it has been shown to participate in the late stages of intra-Golgi protein transport (Ishida et al., 2002). A selenium-binding protein was abundant in young nodules of *L. japonicus* and had also been noted in soybean (Flemetakis et al., 2002). Glyceraldehyde 3-phosphate dehydrogenase (spots 40 and 41) has also been shown to bind selenium in *Escherichia coli* (Lacourciere et al., 2002) and humans (Ogasawara et al., 2005).

### 2.11. Carbon metabolism

Carbon metabolism was the largest group of identified proteins and included enolase (spots 1 and 2), NADP-isocitrate dehydrogenase (spots 11 and 31) sucrose synthase (spot 22), phosphoglycerate kinase (spots 24 and 25) isoflavone reductase (spot 36), 4-coumarate-CoA ligase (spot 37), NAD-glyceraldehyde 3-phosphate dehydrogenase (spots 40, 41, and 52), malate dehydrogenase (spot 46) α-carboxyltransferase (spots 60), and β-amylase (spots 13 and 64). Most of these proteins can be considered as primary metabolic enzymes except isoflavone reductase and 4-coumarate-CoA ligase which are enzymes of secondary metabolism. Isoflavone reductase (spot 36) is an enzyme involved in the biosynthesis of the phytoalexin, medicarpin, that is constitutively found in roots and nodules and inducible in leaves in *Medicago* (Lopez-Meyer and Paiva, 2002). 4-Coumarate-CoA ligase occurs at a branch point from general phenylpropanoid metabolism to several major branch pathways. Interestingly, a number of proteins participating in benzoate and/or phenylpropanoid metabolism were identified in *B. japonicum* bacteroids including anthranilate phosphoribosyl transferase, 2-hydroxyhepta-2,4-diene-1,7-dioate isomerase, phenyl hydroxylase, phospho-2-dehydro-3-deoxyheptonate aldolase and several cytochrome P450 oxygenases (Sarma and Emerich, 2005). These results permit speculation that benzoates and phenylpropanoids may be major carbon sources synthesized by the plant and transported to the bacteroid to provide energy for symbiotic nitrogen fixation.

Isocitrate dehydrogenase and malate dehydrogenase are enzymes of the citric acid cycle. The annotation of isocitrate dehydrogenase as an NADP-dependent enzyme suggests a mitochondrial localization, but it was not detected in either soybean root or nodule mitochondria proteomes (Hoa et al., 2004). Miller et al. (1998) identified a cytosolic and an nodule-enhanced malate dehydrogenase in alfalfa and Appels and Haaker (1988) found multiple malate dehydrogenase activities in the cytosol of pea. Hoa et al. (2004) reported two different malate dehydrogenases found both in root and nodule mitochondria. The soybean nodule mitochondrial enzyme was reported previously (Waters et al., 1985) and here the cytosolic malate dehydrogenase was purified and the peroxisomal enzyme was isolated. Many of the biochemical properties of the mitochondrial, cytosolic and peroxisomal soybean root nodule malate dehydrogenases were found to be similar (data not shown). The lack of inhibition by *p*-hydroxymercuribenzoate clearly differentiated the cytosolic, organellar and bacteroid malate dehydrogenases, and demonstrated the purified malate dehydrogenase from the cytosol was not organellar or bacteroid in origin (Fig. 2). The soybean nodule cytosol malate dehydrogenase had Michaelis constants [L-malate, 8.7 ± 0.7 mM; oxaloacetate, 71 ± 6 μM; $NAD^+$, 808 μM ± 93; NADH, 42 ± 3 μM] similar to those of the nodule-enhanced enzyme from alfalfa (Miller et al., 1998). Tryptophan composition of the purified proteins indicated 8–10 tryptophans per cytoplasmic malate dehydrogenase (4–5 per subunit) and <0.2 tryptophans per mitochondrial dehydrogenase. The lack of tryptophan residues in the peptide fragments identified via mass spectrometry suggests the identified protein was mitochondrial in origin (spot 46).

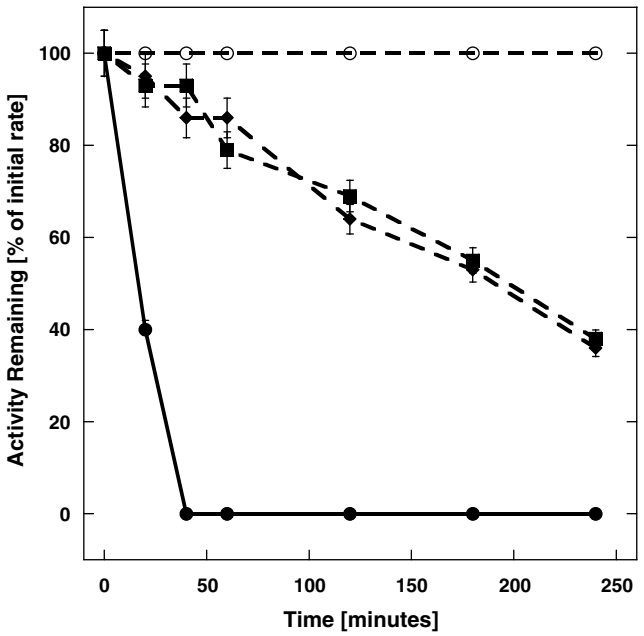


**Fig. 2.** Inhibition of soybean root nodule malate dehydrogenases by *p*-hydroxy mercuribenzoate. Each enzyme was incubated in the inhibitor for the indicated time with 10 mM inhibitor and assayed for activity at the indicated time. One of three replicated experiments is shown. Values represent the mean plus the standard deviations. Source of malate dehydrogenase: cytosolic, ○; bacteroid, ●; mitochondrial, ♦; peroxysome, ■.

Sucrose synthase (spot 22) catalyzes the cleavage of sucrose to fructose and UDP-glucose. Anthon and Emerich (1990) described the operation of the sucrose synthase pathway in soybean nodules. The advantage of the sucrose synthase pathway in nodule metabolism is that it requires three ATPs for the metabolism of sucrose to triose-phosphates as opposed to four ATPs via the invertase pathway (Huber and Akazawa, 1986).

Three of the four enzymes in the 3-carbon segment of glycolysis, glyceraldehyde 3-phosphate dehydrogenase, (spots 40, 41, 52, and 65) phosphoglycerate kinase (spots 24 and 25) and enolase (spots 1 and 2), were among the most abundant proteins in the plant fraction of soybean nodules (Fig. 1). Phosphoglycerate mutase, the remaining enzyme of the 3-carbon segment of glycolysis was not identified as part of this limited proteome search; but it was possible that it was one of the unknown proteins found in this survey as it is not well represented in annotated genomes and libraries. Sucrose synthase, hexokinase, phosphofructokinase, glyceraldehyde-3-phosphate dehydrogenase, phosphoglycerate kinase all have been reported to be more abundant in the uninfected cells (Kouchi et al., 1988; Zammit et al., 1992).

The activities of all four enzymes of the 3-carbon segment of glycolysis were measured in cell-free extracts and found to correlate with nitrogen fixation (Figs. 3 and 4). Kinetic experiments with phosphoglycerate mutase and enolase, indicated that not only

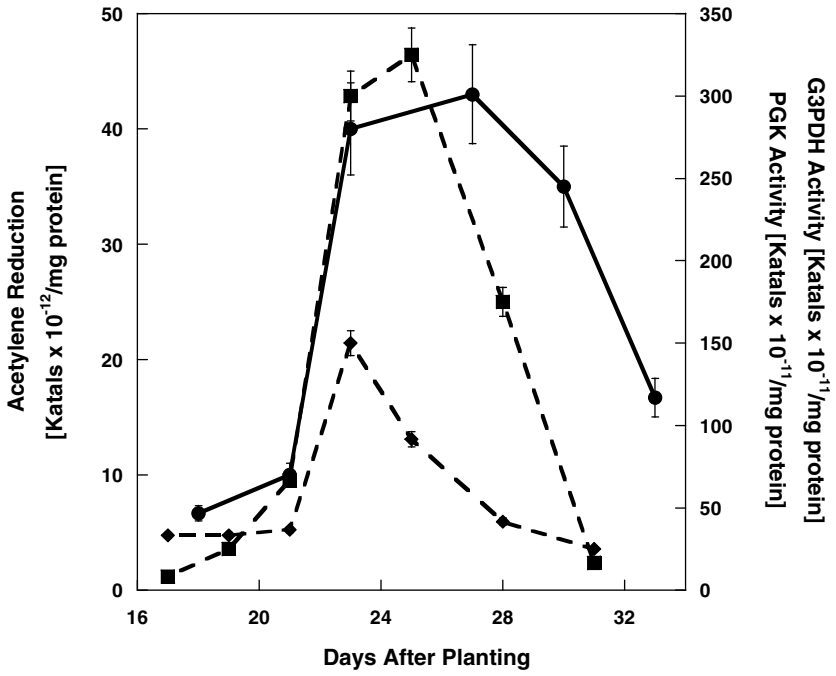


**Fig. 3.** Acetylene reduction, glyceraldehyde 3-phosphate dehydrogenase and phosphoglycerate kinase activities of soybean nodules as a function of plant age. One of three replicated experiments is shown. Values represent the mean plus the standard deviations. Acetylene reduction (●) was performed on whole nodulated root segments. Glyceraldehyde 3-phosphate dehydrogenase (■) and phosphoglycerate kinase (♦) activities were measured in extracts of soybean nodule cytosol.

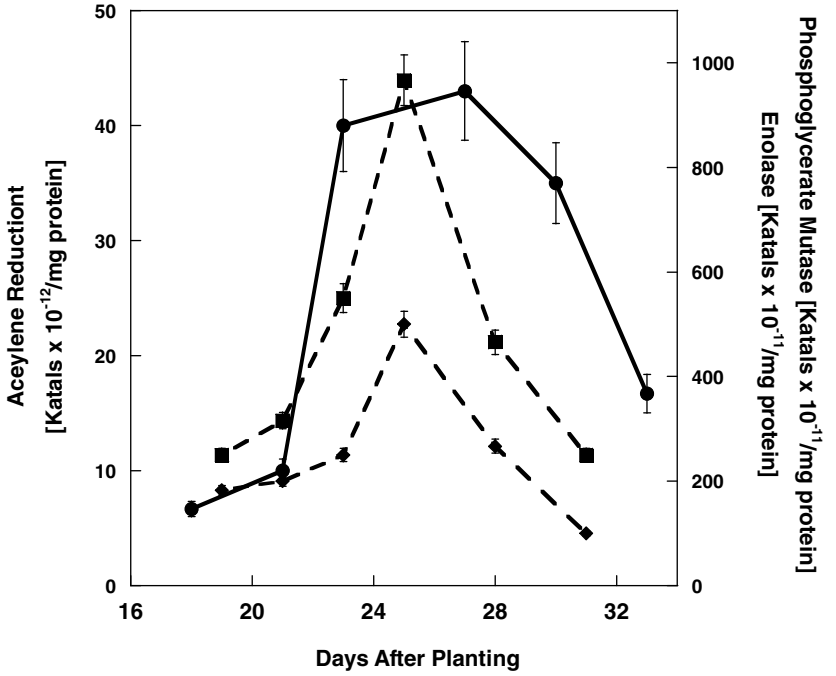


**Fig. 4.** Acetylene reduction, phosphoglycerate mutase and enolase activities of soybean nodules as a function of plant age. One of three replicated experiments is shown. Values represent the mean plus the standard deviations. Acetylene reduction (●) was performed on whole nodulated root segments. Phosphoglycerate mutase (■) and enolase (♦▲) activities were measured in extracts of soybean nodule cytosol.

were their activities substantial but their Michaelis constants ($K_m$) were very low in the direction of PEP synthesis. Phosphoglycerate mutase had a $K_m$ in the range of 250 μM for 3-phosphoglycerate and enolase had a $K_m$ in the range of 150 μM for 2-phosphoglycerate.

## 3. Summary

Approximately half of all the predominate proteins identified in the soybean root nodule cytosol could be classified as involved in carbon and nitrogen metabolism. Another major portion could be

classified as involved in oxygen supply, maintenance and protection. These three groups encompass the major functions of leguminous nitrogen-fixing nodules. Among the abundant proteins was a group involved in vesicular transport suggesting that large macromolecules are actively transported in addition to smaller carbon and nitrogen metabolites. The identification of the proteins of the three carbon portion of glycolysis complete the pathway by which sucrose is provided to the bacteroid as malate. The sucrose synthase pathway (Anthon and Emerich, 1990) and phosphoenolpyruvate carboxylase (Schuller and Werner, 1993) had been characterized previously, but the three carbon portion of the pathway had been assumed but not shown to be correlated with nitrogen fixation activity. The combined proteomic data from the bacteroid, soybean nodule cytosol and mitochondria, and the transcriptomic data provide a consistent pattern of nodule function, but also raises several questions. The most obvious anomaly is that the abundance of membranes in soybean nodules would imply an active and continuous need for their biosynthesis, repair and maintenance. Proteomic analysis of the bacteroid showed a paucity of proteins associated with fatty acid and lipid metabolism (Sarma and Emerich, 2005, 2006) and the same was found in the soybean nodule cytosol proteome. Furthermore, no transcripts were reported for fatty acid or lipid metabolism (Lee et al., 2004). Apparently, the proteins needed for membrane synthesis and function are not highly expressed nor represented as abundant proteins.

## 4. Experimental

### 4.1. Strains of B. japonicum

The *B. japonicum* strains used were USDA 110 (Green and Emerich, 1997) for proteomic analysis and 2143, a rifampicin and nalidixic acid resistant derivative of USDA 3I1B-143 for malate dehydrogenase isolation (Karr and Emerich, 1989).

### 4.2. Soybean seed germination and growth

Soybean seed (*Glycine max* [L] cultivar Williams 82) were surface sterilized as described previously and handled under microbiologically-controlled conditions (Oehrle et al., 2000). Greenhouse plants were grown under 16 h light, 8 h dark using natural and supplemental lighting. Greenhouse plants were grown using a soil-free system of perlite:vermiculite:peat (1:1:1) in a modified hydroponic system and watered with nitrogen-free nutrient solution (Ahmed and Evans, 1960) provided from below via a wicking system (Karr et al., 1984).

### 4.3. Soybean nodule cytosol isolation

Nodules were harvested from 4 week-old greenhouse grown cv. Williams 82 soybean inoculated with *B. japonicum* 110 or 2143. Nodulated soybean roots were removed from the planting media and immediately placed in ice. Nodules were kept cold from the time of harvest through the initial extraction.

Extraction buffers were pre-chilled to 4 °C and equipment was pre-chilled to −20 °C. Large quantities of nodules for protein isolation were ground intermittently (to avoid excessive heat) in a sterilized stainless steel Waring blender. Initial extraction buffer for protein isolation contained 1/3 g insoluble PVP per gram nodule and 2 mL extraction buffer (100 mM Tris–HCl, pH 8.8; 17% w/v sucrose, 100 mM DTT, 1 mM PMSF, 10 mM EDTA, 1 μM pepstatin A, 10 mM leupeptin and 100 μg $mL^{-1}$ benzamidine HCl) per gram nodule. Small quantities of nodules were used for enzymatic analysis and were macerated quickly in a pre-chilled (−20 °C) mortar and pestle.

Macerated nodules were passed through four layers of cheesecloth (pre-moistened with extraction buffer) into a sterile centrifuge tube and centrifuged at 400*g* for 10 min. The supernatant was collected and stored on ice. The resulting pellet was re-extracted twice with the initial extraction buffer, centrifuged at 400*g* for 10 min. to separate the soluble protein fraction (still containing bacteroids) from the insoluble protein fraction. The combined supernatants containing the soluble plant proteins and bacteroids were then spun at 8000*g* for 20 min to pellet the bacteroids. The clarified supernatant was used for electrophoretic separation or analyzed for enzyme activity.

### 4.4. Protein extraction from nodules for electrophoresis

The clarified supernatant was combined 1:1 with Tris-saturated phenol, pH 8.8 and after 30 min of gentle mixing at 4 °C, centrifuged at 8000*g* for 10 min for both one-dimensional or two-dimensional electrophoretic analysis. The upper aqueous fraction was back-extracted once with an equal volume of Tris-saturated phenol and the lower phenolic fraction was extracted twice with an equal volume of 100 mM Tris–HCl, pH 8.8. Five volumes of MeOH containing 100 mM ammonium acetate and 10 mM DTT (chilled to −80 °C) were added to the pooled phenolic fractions and precipitated for 2 h at −80 °C. The solution now containing the precipitated proteins was centrifuged at 4000*g* for 30 min. The resulting pellet was then resuspended and washed twice with several volumes of ice-cold MeOH containing 100 mM ammonium acetate and 10 mM DTT, then twice with several volumes of ice-cold acetone–$H_2O$ (4:1, v/v) with 10 mM DTT. Between each wash and prior to centrifugation at 16,000*g* for 10 min, the solution was placed at −20 °C for 20 min. After the final aq. acetone wash, the protein pellet was dried at 25 °C for approximately 20 min to remove residual acetone, just prior to adding the IEF sample buffer.

The pellet from the initial 400g centrifugation of the macerated nodules was dissolved in a minimal volume of 8.3 M urea, 2 M thiourea, 2% SDS and 100 mM DTT, vortexed heavily for several minutes and centrifuged at 8000*g* for 10 min. The pellet was extracted three times using denaturing buffer with centrifugations of 8000*g* for 10 min between extractions. The supernatants from each extraction were pooled and four volumes of ice-cold acetone–$H_2O$ (4:1, v/v) containing 10 mM DTT were added for a 2 h precipitation at −20° C. The protein precipitate was pelleted at 4000*g* for 30 min and washed three times with several volumes of ice-cold acetone–$H_2O$ (4:1, v/v) containing 10 mM DTT. Between each wash and prior to centrifugation at 16,000*g* for 10 min, the solution was placed at −20 °C for 20 min. After the final wash, the protein pellet was dried at 25 °C for 20 min to remove residual acetone, then the IEF sample buffer was added prior to isoelectric focusing.

### 4.5. Protein extraction from nodules for enzymological analysis

Nodules were harvested quickly, and kept on ice throughout extraction. For whole nodule cytosol, the clarified supernatant (bacteroids removed), was subjected to repeated centrifugal filtration (10,000 MWCO) using 50 mM Tris–Cl, pH 8.0.

### 4.6. Purification of cytosolic malate dehydrogenase

Cytosolic malate dehydrogenase was purified quickly in the presence of protease inhibitors. Nodules (usually 100 g) were ground in 50 mM phosphate buffer (150 mL, pH 7.5), containing 1 mM potassium caproic acid, 1 mM benzamidine, 0.1 mL PMSF, 0.01 mM leupeptin, 0.01% $NaN_3$, 10 mM EDTA and 17% sucrose.

The crude cytosolic fraction obtained after differential centrifugation to remove bacteroids and mitochondria (Waters et al., 1985) was absorbed onto a RedA (Sigma) affinity column and eluted with 50 mM phosphate buffer, pH 7.5, containing 4 M NaCl and 1 mM NADH. The fractions containing malate dehydrogenase activity were concentrated and dialyzed against 50 mM triethanolamine [TEA] buffer, pH 7.5, and then applied to a MonoQ 10/10 FPLC column and eluted with a 0–300 mM NaCl gradient in 50 mM TEA, pH 7.5. Fractions of cytosolic malate dehydrogenase activity were pooled and concentrated in an Amicon concentrator and placed on a Superose 12/12 column equilibrated with 25 mM TEA buffer, pH 7.5. Fractions containing activity were brought to 1.7 M $(NH_4)_2SO_4$ in 50 mM TEA buffer, pH 7.5, and loaded onto a Phenyl Superose column and developed with a 50-0% $(NH_4)_2SO_4$ gradient. The cytosolic malate dehydrogenase activity eluted at ~30% $(NH_4)_2SO_4$. The salt was removed by ultrafiltration. *B. japonicum* bacteroid and soybean nodule mitochondrial malate dehydrogenases were purified as described (Waters et al., 1985).

### 4.7. Tryptophan content of malate dehydrogenase

The tryptophan content of malate dehydrogenase was determined as described by Ghiron et al. (1990).

### 4.8. Peroxisome isolation

Peroxisomes were isolated and extracts prepared as described by Rapp and Randall (1980).

### 4.9. Isoelectric focusing

Isolated proteins for two-dimensional electrophoretic separation were prepared as described above. Proteins were precipitated, washed, and suspended in a minimal volume of IEF sample buffer (8 M urea, 2 M thiourea, 4% w/v CHAPS, 2% v/v Triton X-100, 1% v/v 3–10 ampholytes and 100 mM DTT). After 1 h of moderately heavy vortexing, the protein solutions were aliquoted into smaller volumes and kept at −20 °C for short term storage or −80 °C for long term storage. Samples were discarded after one freeze–thaw cycle (Hopkinson et al., 2005). Protein concentrations were determined, with BSA as standard, using either the method described by Bradford (1976), or the EZQ Protein Quantification Kit (Molecular Probes Inc., Eugene, OR, USA). Protein samples were brought to the appropriate rehydration volume for the corresponding IPG strip using fresh rehydration buffer (7 M urea, 2 M thiourea, 5% w/v CHAPS) containing 130 mM 2-hydroxyethyldisulfide. The concentration of DTT in the rehydration volume was adjusted to obtain a final concentration of 60 mM. The concentration of Triton X-100 was adjusted to obtain 2% v/v for the final rehydration volume of the strip, as were the corresponding ampholytes (IPG buffer; Amersham Biosciences Corp., Piscataway, NJ, USA) to obtain 1% v/v of the final rehydration volume. After gentle vortexing at 25 °C for 30 min., the rehydration buffer was incubated for at least one hour at 4 °C.

Prior to strip rehydration, the sample was centrifuged at 16,000*g* for 20 min. at 12 °C to remove insoluble proteins. The sample was then immediately applied to the IPG strip and allowed to sit in contact with the rehydration solution at 25 °C for 45 min prior to being covered with mineral oil. After a total passive rehydration time of 12–16 h, the strip was placed in a Protean II IEF focusing cell (Bio-Rad Laboratories, Hercules, CA, USA) with premoistened wicks covering each electrode and focused at 12 °C. Two short desalting steps (250 V fast ramp, 250 Vhrs; 1000 V fast ramp, 500–1000 Vhrs) and ramping step (1000 V to final voltage, 2 hours) were included in the custom program. All programs ran at 1.5 times the recommended focusing total Vhrs as reported by the IPG strip manufacturer. At the conclusion of focusing, each strip was removed, mineral oil removed and either stored at −80 °C or immediately incubated separately for 20 min in SDS equilibration buffer (50 mM Tris–HCl, pH 8.8; 6 M urea, 5% w/v SDS, 30% v/v glycerol) containing first 2% w/v DTT, then for 20 min in SDS equilibration buffer containing 2.5% w/v iodoacetamide and then resolved on a second dimension gel.

### 4.10. Second dimension SDS–PAGE

The gradient resolving gels (0.375 M Tris–HCl, pH 8.8; 10–18% T, 0.1% SDS) for the second dimensions were run using the Ettan Dalt*six* Electrophoresis System (Amersham Biosciences). Following polymerization of the resolving gel, a thin stacking gel (0.125 M Tris–HCl, pH 6.8; 5.7% T, 0.1% SDS) was applied and overlaid with gel storage solution (0.125 M Tris–HCl, pH 6.8 containing 0.1% w/v SDS) and allowed to polymerize overnight. Prior to loading the IPG strip, the storage solution was removed and replaced with SDS–PAGE running buffer (0.025 M Tris–HCl, pH 8.3; 0.192 M glycine and 0.1% SDS). The strip and marker protein plug were sealed in with a warm 1% w/v high-melt agarose solution dissolved in SDS–PAGE running buffer. The upper and lower chamber buffers also contained SDS–PAGE running buffer (25 mM Tris, pH 8.3, 192 mM glycine and 0.1% SDS).

The Ettan Dalt*six* gels, 24 cm IPG strips, were run for 6 h at 12 W per gel (constant power, 600 V and 60 mA per gel max.) after an initial 30 min at 5 W per gel. Following the second dimension, gels for image analysis were removed from the cassette and soaked in ultrapure water for 10 min, then fixed for 1 h in MeOH:$H_2O$:$A_2OH$ (5:4:1, v/v) and finally rinsed twice in ultrapure $H_2O$ for 5 min each rinse. Gels for protein analysis were removed from the cassette and soaked in ultrapure water for 10 min, then put directly into staining solution. Gels were stained 16–20 h in Coomassie protein stain (EtOH–$H_2O$ (1:4, v/v), 8% w/v ammonium sulfate, 0.08% w/v Coomassie CB G-250 and 0.35 M phosphoric acid). Gels were destained for 24 h with several changes of ultrapure $H_2O$ using mild shaking. Once destaining was complete, gels were stored in MeOH:ultrapure $H_2O$ (1:4, v/v).

### 4.11. 2D separated protein spot acquisition and analysis

Individual spots were hand picked with a 1.5 mm Spot Picker (The Gel Company, San Francisco, CA, USA), placed in a 96-well ZipPlate and prepared for sequencing using the Montage In-Gel Digest$_{ZP}$ Kit (Millipore Corp., Bedford, MA, USA). Eluted peptide fragments were collected in 96-well v-bottom polypropylene Costar plates (Corning Inc., Corning, NY, USA), spun down to near dryness using a centrivap, and 0.5 μL spotted onto a 96-sample MALDI plate using the ABI Symbiot I robotic liquid handling instrument (Applied Biosystems, Foster City, CA, USA). To each spot was added 0.5 μL of α-cyano-4-hydroxycinnamic acid matrix (10 mg/mL dissolved in $CH_3CN$–$H_2O$ (6:4, v/v) and 0.3% $CF_3CO_2H$). Spots were then allowed to dry completely and loaded into a Voyager DE-Pro MALDI-TOF mass spectrophotometer (Applied Biosystems Inc.) to acquire peptide mass data. Peptide mass fingerprints were analyzed using Mascot (Matrix Science Ltd., www.matrixscience.com) and Protein Prospector (University of California, San Francisco, www.prospector.ucsf.edu) (Clauser et al., 1999). Proteins that satisfied at least three of the following criteria were considered as confidently identified: [1] a minimum of four peptides masses with less than 100 ppm of mass tolerance with the theoretical mass of the peptides, [2] sequence coverage >10% for large proteins and >15% for small proteins, [3] should be the most probable listed protein with a MOWSE score > 500, or a significant MASCOT score and [4] must have congruence, ±10%, between the predicted

theoretical and observed molecular mass and p*I*. Mascot scores are reported as the ratio of the largest probability score observed relative to the minimum probability score to validate identity.

### 4.12. Image acquisition

Coomassie stained gel images were acquired using a UMAX PowerLook 2100XL scanner linked with Adobe Photoshop 7.0. Scanned images were analyzed using the Phoretix 2D Advanced v6.01 software (Nonlinear Dynamics Ltd., Newcastle upon Tyne, UK). Protein quantification using the EZQ kit were acquired using a FujiFilm FLA-5000 and Fuji Image Reader v3.0 software and analyzed using Fuji Multi Gauge v2.3 software (Fuji Photo Film Co., Ltd., Tokyo, Japan).

### 4.13. Enzyme assays

Spectrophotometric enzyme assays were performed using a Cary Bio-1 Spectrophotometer utilizing a multi-cuvette, automated movable block controlled by Cary/Varian endpoint and kinetics software. All assays were performed at 25 °C using high quality reagents diluted in ultrapure water or solvents. The glyceraldehyde 3-phosphate dehydrogenase (EC 1.2.1.12) assay, monitored at $A_{340}$, contained 50 mM HEPES–KOH, pH 8.0; 10 mM $MgCl_2$, 10 mM $KAsO_4$, 1 mM glyceraldehye-3-phosphate, 5 mM DTT, 1 mM $NAD^+$ (Anthon and Emerich, 1990). The phosphoglycerate kinase (EC 2.7.2.3) assay, monitored at $A_{340}$, contained 50 mM HEPES–KOH, pH 8.0; 10 mM 3-phosphoglycerate, 1 mM EDTA, 5 mM DTT, 2.2 mM ATP, 0.2 mM NADH, 5 U $mL^{-1}$ G3PDH (Grattinger et al., 1998). The phosphoglycerate mutase (EC 5.4.2.1) assay, monitored at $A_{240}$, contained 50 mM HEPES–KOH, pH 8.0; 10 mM $MgCl_2$, 50 mM KCl, 5 mM 3-phosphoglycerate, 5 U $mL^{-1}$ enolase (Grana et al., 1989; Grisolia and Carreras, 1975). Enolase (EC 4.2.1.11) assay, monitored at $A_{240}$, contained 50 mM HEPES–KOH, pH 8.0; 10 mM $MgCl_2$, 50 mM KCl, 5 mM 2-phosphoglycerate (Cardenas and Wold, 1971; Sharma and Rothstein, 1979). Cytoplasmic malate dehydrogenase was assayed in 50 mM sodium phosphate, pH 8.0, with other conditions the same as described by Waters et al. (1985). Peroxisomal malate dehydrogenase was assayed by the same procedure as that for mitochondrial malate dehydrogenase (Waters et al., 1985).

## Acknowledgements

We acknowledge the help of Brian Mooney and Beverly DaGue at the University of Missouri Proteomics Core Facility and the support of USDA Grant CREES 2004-25604-14708.

## References

Ahmed, S., Evans, H.J., 1960. Cobalt: a micronutrient element for the growth of soybean plants under symbiotic conditions. Soil Sci. 90, 205–210.

Appels, M.A., Haaker, H., 1988. Identification of cytoplasmic nodule-associated forms of malate dehydrogenase involved in symbiosis between *Rhizobium leguminosarum* and *Pisum sativum*. Eur. J. Biochem. 171, 515–522.

Anthon, G.E., Emerich, D.W., 1990. Developmental regulation of enzymes of sucrose and hexose metabolism in effective and ineffective soybean nodules. Plant Physiol. 92, 346–351.

Bestel-Corre, G., Dumas-Gaudot, E., Poinsot, V., Dieu, M., Dierick, J-F., van Tuinen, D., Remacle, J., Gianinazzi-Pearson, V., Gianinazzi, S., 2002. Proteome analysis and identification of symbiosis-related proteins from *Medicago truncatula* Gaertn. by two-dimensional electrophoresis and mass spectrometry. Electrophoresis 23, 122–137.

Bradford, M.M., 1976. A rapid and sensitive method for the quantitation of microgram quantities of protein utilizing the principle of protein–dye binding. Anal. Biochem. 72, 248–254.

Brodsky, F.M., Chen, C.Y., Knuehl, C., Towler, M.C., Wakeham, D.F., 2001. Biological basket weaving: formation and function of clathrin-coated vesicles. Ann. Rev. Cell Dev. Biol. 17, 517–568.

Brown, S.M., Walsh, K.B., 1994. Anatomy of the legume nodule cortex with respect to nodule permeability. Aust. J. Plant Physiol. 21, 49–68.

Catalano, C.M., Lane, W.S., Sherrier, D.J., 2004. Biochemical characterization of symbiosome membrane proteins from *Medicago truncatula* root nodules. Electrophoresis 25, 519–531.

Cardenas, J.M., Wold, F., 1971. Comparative studies on structural and catalytic properties of enolases. Arch. Biochem. Biophys. 144, 663–672.

Cheon, C-I., Lee, N-G., Siddique, A.B.M., Bal, A.K., Verma, D.P.S., 1993. Roles of plant homologs of Rab7p in biogenesis of peribacteroid membrane, a subcellular compartment formed *de novo* during root nodule symbiosis. EMBO J. 12, 4125–4135.

Clauser, K.R., Baker, P.R., Burlingame, A.L., 1999. Role of accurate mass measurement (+/− 10 ppm) in protein identification strategies employing MS or MS/MS and database searching. Anal. Chem. 71, 2871–2882.

Colebatch, G., Desbrosses, G., Ott, T., Krusell, L., Montanari, O., Koska, S., Kopka, J., Udvardi, M.K., 2004. Global changes in transcripton orchestrate metabolic differentiation during symbiotic nitrogen fixation in *Lotus japonicus*. Plant J. 39, 353–362.

Dalton, D.A., Baird, L.M., Langeberg, L., Taugher, C.Y., Anyan, W.R., Vance, C.P., Sarath, G., 1993. Subcellular localization of oxygen defense enzymes in soybean (*Glycine max* [L.] Merr.) root nodules. Plant Physiol. 102, 481–489.

Decker, B.L., Wickner, W.T., 2006. Enolase activates homotypic vacuole fusion and protein transport to the vacuole in yeast. J. Biol. Chem. 281, 14523–14528.

El Yahyaoui, F., Kuster, H., Ben Amor, B., Hohnjec, N., Puler, A., Becker, A., Gouzy, J., Vernie, T., Gough, C., Neibel, A., Godiard, L., Gamas, P., 2004. Expression profiling in *Medicago truncatula* identifies more than 750 genes differentially expressed during nodulation, including many potential regulators of the symbiotic program. Plant Physiol. 136, 3159–3176.

Farmer, E.E., 1994. Fatty acid signaling in plants and their associated microorganisms. Plant Mol. Biol. 26, 1423–1437.

Flemetakis, E., Agalou, A., Kavroulakis, N., Dimou, M., Martsikovaskaya, A., Slater, A., Spaink, H.P., Roussis, A., Katinakis, P., 2002. *Lotus japonicus* gene *Ljsbp* is highly conserved among plants and animals and encodes a homologue to the mammalian selenium-binding proteins. Mol. Plant–Microbe Interact. 15, 313–322.

Ghiron, C.A., Eftinck, M.R., Waters, J.K., Emerich, D.W., 1990. Fluorescence studies with malate dehydrogenase from *Bradyrhizobium japonicum* 3I1b–143 bacteroids: a two tryptophan-containing protein. Arch. Biochem. Biophys. 283, 102–106.

Gordon, A.J., Thomas, B.J., Reynolds, P.H.S., 1992. Localization of sucrose synthase in soybean nodules. New Phytol. 122, 35–44.

Grana, X., Urena, J., Ludevid, D., Carreras, J., Climent, F., 1989. Purification, characterization and immunological properties of 2,3-bisphosphateglycerate-independent phosphoglycerate mutase from maize (*Zea mays*) seeds. Eur. J. Biochem. 186, 149–153.

Grattinger, M., Dankesreiter, A., Schurig, H., Jaenicke, R., 1998. Recombinant phosphoglycerate kinase from the hyperthermophilic bacterium *Thermotoga maritima*: catalytic, spectral and thermodynamic properties. J. Mol. Biol. 280, 525–533.

Green, L.S., Emerich, D.W., 1997. *Bradyrhizobium japonicum* does not require α-ketoglutarate dehydrogenase for growth on succinate or malate. J. Bacteriol. 179, 94–201.

Grisolia, S., Carreras, J., 1975. Phosphoglycerate mutase from wheat germ (2,3-PGA-independent). Meth. Enzymol. 42, 425–438.

Hoa, L.T-P., Nomura, M., Kajiwara, H., Day, D.A., Tajima, S., 2004. Proteomic analysis on symbiotic differentiation of mitochondria in soybean nodules. Plant Cell Physiol. 45, 300–308.

Hopkinson, A., McIntosh, R.S., Layfield, R.J., Keyte, J., Dua, H.S., Tighe, P.J., 2005. Optimised two-dimensional electrophoresis procedures for the protein characterisation of structural tissues. Proteomics 5, 1–13.

Huber, S.C., Akazawa, T., 1986. A novel sucrose synthase pathway for sucrose degradation in cultured sycamore cells. Plant Physiol. 81, 1008–1013.

Ishida, T., Ishii, Y., Yamada, H., Oguri, K., 2002. The induction of hepatic selenium-binding protein by aryl hydrocarbon (Ah)-receptor ligands in rats. J. Health Sci. 48, 62–68.

Larrainzar, E., Wienkoop, S., Weckman, W., Ladrera, R., Arrese-Igor, C., Gonzáles, E.M., 2007. *Medicago truncatula* root nodule proteome analysis reveals differential plant and bacteroid responses to drought stress. Plant Physiol. 144, 1495–1507.

Junghans, T.G., de Almeida-Oliveira, M.G., Moreira, M.A., 2004. Lipoxygenase activities during development of root and nodule of soybean. Pesq. Agropec. Bras. 39, 625–630.

Jürgens, G., 2004. Membrane trafficking in plants. Ann. Rev. Cell Dev. Biol. 20, 481–504.

Karr, D.B., Waters, J.K., Suzuki, F., Emerich, D.W., 1984. Enzymes of the poly-3-hydroxybutyrate and citric acid cycles of *Rhizobium japonicum* bacteroids. Plant Physiol. 75, 1158–1162.

Karr, D.B., Emerich, D.W., 1989. Protein phosphorylation in *Bradyrhizobium japonicum* bacteroids and cultures. J. Bacteriol. 171, 3420–3426.

Kersten, B., Burkle, L., Eckehard, J.K., Giavalisco, P., Konthur, Z., Lueking, A., Walter, G., Eickhoff, H., Schneider, U., 2002. Large-scale plant proteomics. Plant Mol. Biol. 48, 133–141.

Kim, J., Dang, C.V., 2005. Multifaceted roles of glycolytic enzymes. Trends Biochem. Sci. 30, 142–150.

Kinnback, A., Mellor, R., Werner, D., 1987. α-Mannosidase II isoenzyme in the peribacteroid space of *Glycine max* root nodules. J. Exp. Bot. 38, 1373–1377.

Kouchi, H., Fukai, K., Katagin, H., Minamisawa, K., Tajima, S., 1988. Isolation and enzymological characterization of infected and uninfected cell protoplasts from root nodules of *Glycine max*. Physiol. Plant. 73, 327–334.

Kouchi, H., Shimomura, K., Hata, S., Hirota, A., Wu, G.J., Kumagai, H., Tajima, S., Suganuma, N., Suzuki, A., Aoki, T., Hayashi, M., Yokoyama, T., Ohyama, T., Asamizu, E., Kuwata, C., Shibata, D., Tabata, S., 2004. Large-scale analysis of gene expression profiles during early stages of root ndoule formaiton in amodel legume, *Lotus japonicus*. DNA Res. 11, 263–274.

Krishnan, H.B., Karr, D.B., Emerich, D.W., 1999. Purification of an autophosphorylating protein from imbibing soybean (*Glycine max* L). seed exudate and its identification as a nucleoside diphosphate kinase. J. Plant Physiol. 154, 584–590.

Lacourciere, G.M., Levine, R.L., Stadtman, T.C., 2002. Direct detection of potential selenium delivery proteins by using an *Escherichia coli* strain unable to incorporate selenium from selenite into proteins. Proc. Natl. Acad. Sci. USA 99, 9150–9153.

Lee, H., Hur, C-G., Oh, C.J., Ho, B.K., Park, S-Y., An, C.S., 2004. Analysis of the root nodule-enhanced transcriptome in soybean. Mol. Cells 18, 53–62.

Leelapon, O., Sarath, G., Staswick, P.E., 2004. A single amino acid substitution in soybean VSPα increases its acid phosphatase activity nearly 20-fold. Planta 219, 1071–1079.

Lin, J., Wood, S., Becana, M., Klucas, R.V., 1991. Purification and characterization of soybean root nodule ferric leghemoglobin reductase. Plant Physiol. 96, 32–37.

Lodwig, E.M., Hosie, A.H.F., Bourdes, A., Findlay, K., Allaway, D., Karunakaran, R., Downie, J.A., Poole, P.S., 2003. Amino-acid cycling drives nitrogen fixation in the legume–*Rhizobium* symbiosis. Nature 422, 722–726.

Lopez-Meyer, M., Paiva, N.L., 2002. Immunolocalization of vestitone reductase and isoflavone reductase, two enzymes involved in the biosynthesis of the phytoalexin medicarpin. Physiol. Mol. Plant Pathol. 61, 15–30.

Memon, A.R., 2004. The role of ADP-ribosylation factor and SAR1 in vesicular trafficking in plants. Biochim. Biophys. Acta 1664, 9–30.

Meuriot, F., Noquet, C., Avice, J-C., Volenec, J.J., Cunningham, S.M., Sors, T.G., Caillot, S., Ourry, A., 2004. Methyl jasmonate alters N partitioning, N reserves accumulation and induces gene expression of a 32-kDa vegetative storage protein that possesses chitinase activity in *Medicago sativa* taproots. Physiol. Plant. 120, 113–123.

Miller, S.S., Driscoll, B.T., Gregerson, R.G., Gantt, J.S., Vance, C.P., 1998. Alfalfa malate dehydrogenase (MDH): Molecular cloning and characterization of five different forms reveals a unique nodule-enhanced MDH. Plant J. 15, 173–184.

Mohammadi, M., Karr, A.L., 2003. Induced lipoxygenases in soybean root nodules. Plant Sci. 164, 471–479.

Mooney, B.P., Thelen, J.J., 2004. High-throughput peptide mass fingerprinting of soybean seed proteins: automated workflow and utility of UniGene expressed sequence tag databases for protein identification. Phytochemistry 65, 33–1744.

Moran, J.F., Sun, Z., Sarath, G., Arredondo-Peter, R., James, E.K., Becana, M., Klucas, R.V., 2002. Molecular cloning, functional characterization, and subcellular localization of soybean nodule dihydrolipoamide reductase. Plant Physiol. 128, 300–313.

Newcomb, E.H., Tandon, S.R., 1981. Uninfected cells of soybean root nodules: Ultrastructure suggests key role in ureide production. Science 212, 1394–1396.

Nguyen, T., Zelechowska, M., Foster, V., Bergmann, H., Verma, D.P.S., 1985. Primary structure of he soybean nodulin-35 gene encoding uricase II localized in the peroxisomes of uninfected cells of nodules. Proc. Natl. Acad. Sci. USA 82, 5040–5044.

Oehrle, N.W., Karr, D.B., Kremer, R.J., Emerich, D.W., 2000. Enhanced attachment of *Bradyrhizobium japonicum* to soybean through reduced root colonization of internally-seedborne microorganisms. Can. J. Microbiol. 46, 600–606.

Ogasawara, Y., Lacourciere, G.M., Ishii, K., Stadtman, T.C., 2005. Characterization of potential selenium-binding proteins in the selenophosphate synthetase system. Proc. Natl. Acad. Sci. USA 102. 10112-1016.

Panter, S., Thomson, R., de Bruxelles, G., Laver, D., Trevaskis, B., Udvardi, M., 2000. Identification of proteomics of novel proteins associated with the peribacteroid membrane of soybean root nodules. Mol. Plant–Microbe Interact. 13, 325–333.

Penheiter, A.R., Duff, S.M.G., Sarath, G., 1997. Soybean root nodule acid phosphatase. Plant Physiol. 114, 597–604.

Rapp, B.J., Randall, D.D., 1980. Pyruvate dehydrogenase complex from germinating castor bean endosperm. Plant Physiol. 65, 314–318.

Roth, E., Jeon, K., Stacey, G., 1988. Homology in endosymbiotic systems: the term "symbiosome". In: Palacios, R., Verma, D.P.S. (Eds.), Molecular Genetics of Plant Microbe Interactions. ADS Press, St. Paul, pp. 220–225.

Sánchez, F., Padilla, J.E., Pérez, H., Lara, M., 1991. Control of nodulin genes in root-nodule development and metabolism. Annu. Rev. Plant Physiol. Plant Mol. Biol. 42, 507–528.

Sarma, A.D., Emerich, D.W., 2005. Global protein expression pattern of *Bradyrhizobium japonicum* bacteroids: a prelude to functional proteomics. Proteomics 5, 4170–4184.

Sarma, A.D., Emerich, D.W., 2006. A comparative proteomic evaluation of culture grown vs nodule isolated *Bradyrhizobium japonicum*. Proteomics 6, 3008–3028.

Schuller, K.A., Werner, D., 1993. Phosphorylation of soybean (*Glycine max* L.) nodule phosphoenolpyruvate carboxylase *in vitro* decreases sensitivity to inhibition by L-malate. Plant Physiol. 101, 1267–1273.

Sharma, H.K., Rothstein, M., 1979. A new method for detection of enolase activity on polyacrylamide gels. Anal. Biochem. 98, 226–230.

Staswick, P.E., 1989. Preferential loss of an abundant storage protein from soybean pods during seed development. Plant Physiol. 90, 1252–1255.

Tesfaye, M., Silverstein, K.A., Bucciarelli, B., Samac, D.A., Vance, C.P., 2006. The Affymetrix Medicago GeneChip Array is applicable for transcript analysis of alfalfa (*Medicago sativa*). Funct. Plant Biol. 33, 783–788.

Tranbarger, T.J., Franceschi, V.R., Hildebrand, D.F., Grimes, H.D., 1991. The soybean 94-kilodalton vegetative storage protein is a lipoxygenase that is localized in the paravenial mesophyll cell vacuoles. Plant Cell 3, 973–987.

Udvardi, M.K., Day, D.A., 1997. Metabolite transport across symbiotic membranes of legume nodules. Annu. Rev. Plant Physiol. Plant Mol. Biol. 48, 493–523.

Van den Bosch, K.A., Newcomb, E.H., 1985. Immunogold localization of nodule-specific uricase in developing soybean root nodules. Planta 167, 425–436.

Vandenbosch, K.A., Newcomb, E.H., 1988. The occurrence of leghemoglobin protein in the uninfected interstitial cells of soybean root nodules. Planta 175, 422–451.

Verma, D.P.S., Hong, Z., 1996. Biogenesis of the peribacteroid membrane in root nodules. Trends Microbiol. 4, 364–368.

Wan, J., Torres, M., Ganapathy, A., Thelen, J., DaGue, B.B., Mooney, B., Xu, D., Stacey, G., 2005. Proteomic analysis of soybean root hairs after infection by *Bradyrhizobium japonicum*. Mol. Plant–Microbe Interact. 18, 458–467.

Waters, J.K., Karr, D.B., Emerich, D.W., 1985. Malate dehydrogenase from *Rhizobium japonicum* 3I1b-143 Bacteroids and *Glycine max* root-nodule mitochondria. Biochemistry 24, 6479–6486.

Wasternack, C., Hause, B., 2002. Jasmonates and octadecanoids – signals in plant stress response and development. In: Moldave, K. (Ed.), Progress in Nucleic Acid Research and Molecular Biology. Academic Press, New York, pp. 165–221.

Wienkoop, S., Saalbach, G., 2003. Proteome analysis. Novel proteins identified at the peribacteroid membrane from *Lotus japonicus* root nodules. Plant Physiol. 131, 1080–1090.

Wittenbach, V.A., 1982. Effect of pod removal on leaf senescence in soybeans. Plant Physiol. 70, 1544–1548.

Winzer, T., Bairl, A., Linder, M., Linder, D., Werner, D., Muller, P., 1999. A novel 53-kDa nodulin of the symbiosome membrane of soybean nodules, controlled by *Bradyrhizobium japonicum*. Mol. Plant–Microbe Interact. 12, 218–226.

Zammit, A., Copeland, L., 1993. Immunocytochemical localisation of nodule-specific sucrose synthase in soybean nodules. Aust. J. Plant Physiol. 20, 25–32.

Zammit, A., Copeland, L., Miller, C., Craig, S., 1992. Immunocytological localization of NAD-dependent glyceraldeyde-3-phosphate dehydrogenase in soybean nodules. Physiol. Plant. 84, 549–594.

Zhang, K., McKinlay, C., Hocart, C.H., Djordjevic, M.A., 2006. The *Medicago truncatula* small protein proteome and peptidome. J. Proteome Res. 5, 3355–3367.

Zuk, M., Prescha, A., Kepxzynski, J., Szopa, J., 2003. ADP ribosylation factor regulates metabolism and antioxidant capacity of transgenic potato tubers. J. Agric. Food Chem. 51, 288–294.